La-Based Material for Energy Storage Applications

F.E. Atalay*, H. Kaya, A. Bingol and D. Asma

Inonu University, Science and Art Faculty, Department of Physics, Malatya 44280, Turkey

In this work, nanostructured La-based materials were produced by chemical precipitation method onto Cladosporium cladosporioides fungal hyphae in aqueous solution. Materials were annealed at various temperatures between $100\,°C$–$600\,°C$. The morphological properties of the synthesized material were studied by transmission electron microscopy. The surface area for sample annealed at $360\,°C$ was determined to be 85.64 m^2/g using Brunauer-Emmett-Teller method. The nitrogen adsorption and desorption isotherm displayed a typical type-IV isotherm. Electrochemical properties of produced material were studied using cyclic voltammetry, long term charge/discharge analysis and impedance spectroscopy in the 0.5 M Na_2SO_4 electrolyte. The obtained nanostructured porous electrode exhibits quasi-rectangular shaped cyclic voltammetry curves with a specific capacitance of 2190 F/g at a scan rate of 2 mV/s.

1. Introduction

Recently, rare earth metal oxide and hydroxide nanomaterials have been extensively investigated because these materials have many potential applications in electronics, optics, catalysis, magnetic data storage, hydrogen storage, automotive industry and biotechnology. Nanomaterials with different sizes and shapes have been synthesized with various methods, such as chemical precipitation, solvothermal, sol-gel and hydrothermal method. However, there are very few studies on preparation and characterization of La-based oxide nanomaterials.

Currently, supercapacitors are one of the most promising energy storage systems. So far, nanostructured metal oxide materials, such as NiO, RuO_2, Co_3O_4 and Mn_xO_y, have been used as a supercapacitor electrode active material. Lanthanum element with its special electron shell structure has obvious influence on the capabilities of many materials [1]. It is well known that La-based oxide nanomaterials have not been reported as electrode active materials.

The surface area of electrode active material is a very important parameter to affect supercapacitor performance. The surface area can be increased using a biotemplate. We have used outer surface of bacteria and fungi as a biotemplate in our earlier work [2–4]. It was reported that especially fungal cell walls can act as cation exchangers, because of their negative charge, which originates from the presence of different functional groups, e.g. carboxylic, phosphate, amine or sulfhydryl groups [5, 6]. The tubular structure of fungi results in high tolerance towards metals, high wall-binding capacity and intracellular metal uptake capabilities, compared to bacterial strains [4].

In this work, for the first time nanostructured La-based metal oxide materials with high surface-to-volume ratio are synthesized using fungus as biotemplate. We have examined their usage in energy storage application as an electrode active material.

2. Materials and equipment

We have used similar methods in our earlier work [4] to produce nanostructured La-based metal oxide. Approximately 50 ml suspension of C. cladosporioides fungus was used as a biotemplate. 500 ml of 0.1 M $La(NO_3)_2$ solution was added to a cell suspension of C. cladosporioides at 10 ml/min, using a Metrohm 807 dosing unit. After shaking the mixture for 30 minutes, 250 ml of 0.1 M $NaBH_4$ solution, used as a reducing agent, was added to the mixture at 10 ml/min using dosing unit. This mixture was shaken at 800 rpm for 24 hours. Then, $La(OH)_3$/fungus precipitate was obtained by centrifugation at 9000 rpm for 15 min. The precipitate was washed twice with deionized water and once with ethanol, subsequently. The $La(OH)_3$/fungus precipitate was dried for 12 hours in a vacuum oven at $60\,°C$ at 600 mmHg pressure. Then, the precipitate was annealed in air atmosphere for 12 hours at temperatures in range between $100\,°C$ and $600\,°C$. Subsequently, the nanostructured La-based materials (75%) and acetylene black (20%) were grinded and mixed in a Zr_2O_3 mortar for 45 min. Then PTFE (5%) was added to mortar. The resultant mixture was grinded again for 60 min. 5 mg of the obtained homogeneous mixture was pressed on Ni foam under a pressure of 10 MPa for 45 min and was used as the working electrode.

A reference electrode was composed of Ag/AgCl (with ceramic frit, ALS, saturated KCl, and 45 mV versus SCE at $20\,°C$). Platinum was used in auxiliary electrodes. All of the electrochemical experiments were carried out in a three-electrode cell configuration in 0.5 M Na_2SO_4. Electrochemical investigations included cyclic voltammetry (CV) measurements, galvanostatic charge-discharge tests and electrochemical impedance spectroscopy (EIS) using a Gamry Reference 3000 potentiostat/galvanostat/ZRA. The electrochemical impedance spectroscopy (EIS) tests

---

*corresponding author; e-mail: funda.atalay@inonu.edu.tr

were conducted with a frequency loop from 100 kHz to 10 MHz with 5 mV AC oscillation amplitude under an open-circuit potential.

The morphology of the La-based materials was characterized by scanning electron microscopy (SEM; JEOL JSM-7001F) and transmission electron microscopy (TEM; JEOL 2100F). Nitrogen adsorption was performed at 77.3 K by means of a Micromeritics Gemini VII 2390t. The surface area was calculated using the BET equation. The pore size distribution was determined by the Barrett-Joyner-Halenda (BJH) method.

Thermogravimetric analysis (TGA) curves and differential thermal analysis (DTA) curves were recorded using a Shimadzu TGA/DTA-50 systems, in air by heating samples from room temperature to 900 °C with a ramp rate of 10 °C/min. The crystal structure and orientation were determined by a Rigaku Ultima-IV X-Ray Diffractometer (XRD) using Cu K_α radiation.

3. Results and discussion

The TG/DTA results of bare fungi and the La-based material on fungi, produced by chemical precipitation at temperatures in range 24 °C–800 °C, are shown in Fig. 1a.
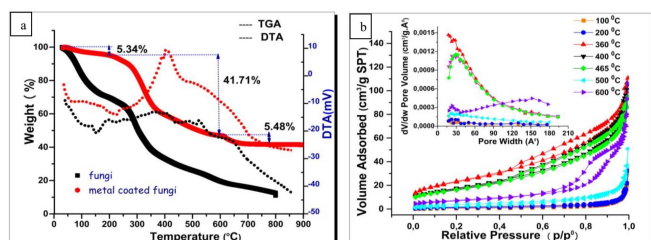

Fig. 1. (a) TGA/DTA measurements of bare fungi and La-coated fungi. (b) Nitrogen adsorption isotherm of nanostructured La-based material, annealed at various temperatures. Inset shows BJH pore size distribution of La-based material.

TGA/DTA measurements were made to determine transition temperatures of $La(OH)_3$ to LaOOH and La_2O_3. The total weight loss at 800 °C for bare fungi and metal coated fungi is 89.02% and 52.53%, respectively. We have recently reported that the steady weight loss from room temperature to 120 °C for bare fungi is due to initial loss of moisture. Subsequent steady weight loss from 120 °C to 290 °C can be attributed to the continual expulsion of water and ethanol from the sample. Final steady weight loss in the temperature range of 290 °C–800 °C can be attributed to fungal degradation [4]. It is seen from TGA curve for metal coated fungi that the weight loss has occurred at three steps. The first step of weight loss is 5.04% at 210 °C. It arises from $La(OH)_3$ to LaOOH transformation and also from simultaneous degradation of the fungi. The next step of gradual weight loss up to 600 °C is of 41.71% and can be attributed to LaOOH to La_2O_3 transformation. The third step of weight loss up to 770 °C is of 5.48%. It is due to removal of nitrate

ion from sample. The endothermic peaks on the DTA curve, appearing at 375 °C and 500 °C, show the decomposition reaction of lanthanum compound. After heating to 375 °C, LaOOH has formed. The peak at approximately 500 °C, suppressed by the first peak, results from La_2O_3 formation.

The specific surface area is a significant microstructural parameter of materials, which depends on the geometrical shape and porosity. It is also well known that a large surface area could be an important factor, improving the electrochemical performance of supercapacitors. Yang et al. [7] have reported that the electrochemical performance can be improved by the hierarchical nanostructural design, integrating the high conductivity and large surface areas of the electrode, to permit homogeneous interface/chemical distributions at the nanoscale and fast ion and electron transfers. Figure 1b shows the BET surface area measurement results for samples annealed in 100 °C–600 °C temperature range. The samples annealed at 360 °C, 400 °C and 465 °C exhibit specific surface area of 85.64, 64.26 and 59.80 m^2/g, respectively. The inset of Fig. 1b shows the BJH desorption pore size distribution curves of annealed samples. We can see that most of the micropores in all samples have a size smaller than 18 nm. The most probable pore size, estimated from the peak position, is about 2.3 nm for the sample annealed at 360 °C. The mesopore structure collapsed above 465 °C due to crystallization of La_2O_3, which results from decrease in surface area and increase in average pore with. The BET surface area of 600 °C annealed sample has reduced to 26.6 m^2/g.
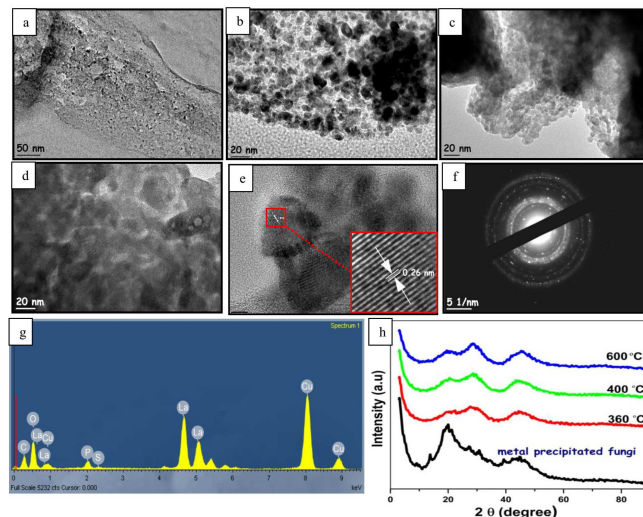

Fig. 2. TEM images of La-based materials, annealed at various temperatures. (a) 100 °C, (b) 360 °C, (c) 400 °C, (d) 600 °C, (e) HRTEM image, (f) SAED pattern, (g) EDS pattern and (h) XRD pattern of the sample annealed at 360 °C.

Figure 2a–d shows the size and morphology of La-based materials produced on fungi. It can be seen that the most nanoporous structure, among the annealed

samples, has the sample annealed at 360 °C (Fig. 2b). The high magnification TEM image of sample annealed at 360 °C shown in Fig. 2e also indicates that the particles are all crystalline and their sizes again fall in the range of 6–20 nm. The spacing between the fringes is about 2.6 Å. Figure 2f shows the corresponding selected area electron diffraction (SAED) pattern. The SAED pattern illustrates the fine grained polycrystalline structure of sample. Figure 2g shows the energy dispersive analysis (EDS) pattern of the sample. The significant peaks around 4.66 keV and 5.05 keV, show the presence of La. To confirm these findings, XRD studies were conducted as shown Fig. 2h. The broad XRD peaks are observed for all samples, which is an exhibition of formation of nanocrystals.
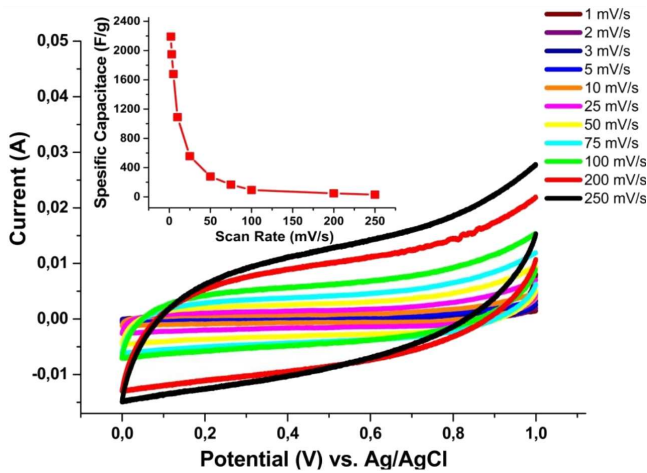

Fig. 3. CV curves of La-based electrodes at different scan rates. The inset shows the specific capacitance as a function of the scan rate.

A quasi-rectangular shape of CV curves shows that the La-based supercapacitor electrode has electrochemical capacitive performance over the potential window between 0 V and 1 V, as shown in Fig. 3. Wand et al. [8] have reported that quasi-rectangular shape of CV arises from unique electrochemical features of electrode active materials, such as reversible redox process, high thermal and chemical stability and pseudo capacitance. The CV curves with same shape at all scan rates also indicate a good capacitive performance of electrode. The specific capacitance was calculated from the CV curves using the following equation:

$$C_{\mathbf{s}} = \frac{\int I \, dV}{s \Delta V m}, \qquad (1)$$

where I is the current, s is the scan rate, ΔV is the potential window and m is the mass of the active material. La-based electrode yielded the maximum specific capacitance of 2190 F/g at 2 mV/s (as shown in the inset of Fig. 3). When the scan rate is changed to 5 mV/s, the specific capacitance of the porous electrode is 93 F/g. It was also observed that the specific capacitance value decreases with increasing scan rate, which is due

to limited ion movement at high scan rates. Specific energy density and power density were also calculated from the the CV curves and are equal to 304.1 Wh/kg and 2190 W/kg, respectively.
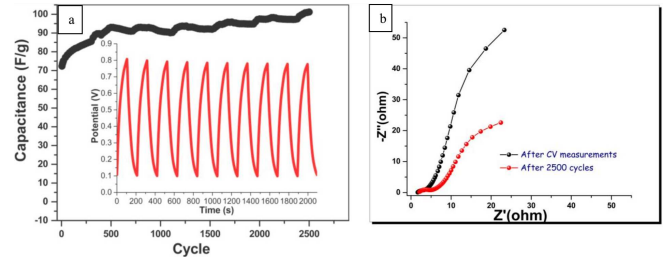

Fig. 4. (a) The variation of specific capacitance as a function of cycle number of La-based electrode. The inset shows the ten cyclic charge-discharge curves. (b) Nyquist plots of La-based electrode at open circuit potential in 1 M Na_2SO_4 electrolyte.

The first ten galvanostatic charge-discharge cycles of nanostructured La-based electrode at current of 0.4 A/g are given in the inset of Fig. 4a. The long term galvanostatic cyclability of the material was investigated over 2500 cycles. The initial capacitance value was 72 F/g. The capacitance value of porous electrode was increasing gradually during the cycling process. After 2500 continuous charge/discharge cycles, it has reached the maximum capacitance value of 102 F/g. This value is in a good agreement with the value obtained from CV curve at scan rate of 5 mV/s. It was also seen that there is no capacitance loss with the increasing number of cycles. This improvement in capacitance of the electrode is the result of the gradual access of electrolyte ions to the active sites of the electrode surface with the continuous cycles [9, 10]. The electrochemical behavior of nanostructured porous electrode was also investigated by EIS. Figure 4b shows the Nyquist plots of symmetric cell after the CV measurements and long-term cycling at an open circuit potential. The visible semicircle in high frequency region is related to the charge transfer resistance R_{ct}, which contributes to the pseudocapacitance. The contact resistance between the electrolyte and the electrode material is approximately 1.67 and 2.11 Ω, before and after the cycle test, respectively, which shows changes by 20%. The estimated R_{ct} value is approximately 3.84 Ω. The sloped line in the low frequency range is associated with the ion diffusion within the electrode surface. After 2500 continuous cycles, an increase of charge transfer resistance in the middle frequency range is observed. The slope of the straight line in the low frequency range has decreased from 70° to 49°.

4. Conclusions

In summary, La-based materials were synthesized with chemical precipitation method onto Cladosporium cladosporioides fungal hyphae. It has been found that the synthesized porous electrode, annealed at 360 °C, exhibits high surface area, high capacitance, long cycle life

and good coulombic efficiency. The results obtained from the electrochemical studies suggest that La-based porous materials could be used as high performance materials for energy storage systems.

Acknowledgments

References

[1] G. Shao, Y. Yao, S. Zhang, P. He, *Rare Metals* **28**, 132 (2009).

[2] F.E. Atalay, D. Asma, H. Kaya, E. Ozbey, *Mater. Sci. Semicon. Process.* **38**, 314 (2015).

[3] F.E. Atalay, H. Kaya, D. Asma, A. Bingol, *Biointerface Res. Appl. Chem.* **6**, 1099 (2016).

[4] F.E. Atalay, D. Asma, H. Kaya, A. Bingoland, P. Yaya, *Nanomater. Nanotechnol.* **28**, 6 (2016).

[5] M. Fomina, J. Charnock, A.D. Bowen, G.M. Gadd, *Environ. Microbiol.* **9**, 308 (2007).

[6] Y.S. Chan, M.M. Don, *Int. Arab. J. Antimicrob. Agents.* **2**, 1 (2012).

[7] Q. Yang, Z. Lu, J. Liu, X. Lei, Z. Chang, L. Luo, X. Sun, *Prog. Nat. Sci.: Mater. Int.* **23**, 351 (2013).

[8] Y. Wang, J. Guo, T. Wang, J. Shao, D. Wang, Y.W. Yang, *Nanomaterials* **5**, 1667 (2015).

[9] J. Candler, T. Elmore, B.K. Gupta, L. Dong, S. Palchoudhury, R.K. Gupta, *New J. Chem.* **39**, 6108 (2015).

[10] Y.F. Yuan, X.H. Xia, J.B. Wu, X.H. Huang, Y.B. Pei, J.L. Yang, S.Y. Guo, *Electrochem. Commun.* **13**, 1123 (2011).